ACS APPLIED MATERIALS & INTERFACES

Research Article

www.acsami.org

Design of Electrical Conductive Composites: Tuning the Morphology to Improve the Electrical Properties of Graphene Filled Immiscible Polymer Blends

Cui Mao,[†,‡] Yutian Zhu,*[,†] and Wei Jiang*[,†]

[†]State Key Laboratory of Polymer Physics and Chemistry, Changchun Institute of Applied Chemistry, Chinese Academy of Sciences, Changchun 130022, P.R. China

[‡]Graduate University of the Chinese Academy of Sciences, Beijing 100049, P.R. China

Supporting Information

ABSTRACT: Polystyrene (PS) and poly(methyl methacrylate) (PMMA) blends filled with octadecylamine-functionalized graphene (GE-ODA) have been fabricated to obtain conductive composites with a lower electrical percolation threshold according to the concept of double percolation. The dependence of the electrical properties of the composites on the morphology is examined by changing the proportion of PS and PMMA. Our results reveal that the electrical conductivity of the composites can be optimal when PS and PMMA phases form a cocontinuous structure and GE-ODA nanosheets are selectively located and percolated in the PS phase. For the PS/PMMA blend (50w/50w), the composites exhibit an extremely low electrical percolation threshold (0.5 wt %) because of the formation of a perfect double percolated structure. Moreover, the rheological properties of the composites are also measured to gain a fundamental understanding of the relationship between microstructure and electrical properties.

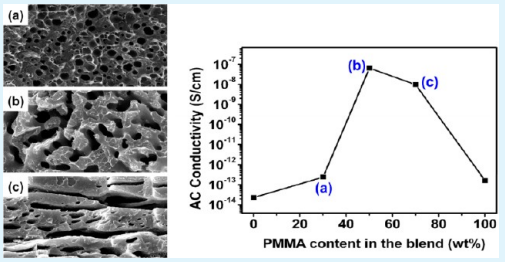

KEYWORDS: *immiscible polymer blends, functionalized graphene, electrical properties, double percolation, rheological properties*

1. INTRODUCTION

Graphene, a monolayer of carbon atoms arranged in a honeycomb network, has attracted great attention due to its excellent mechanical,[1] thermal,[2] and electrical properties[3] as well as its potential use in various fields, such as electronics,[4] supercapacitors,[5,6] and sensors.[7] Recently, graphene has been added into a host of polymers to produce conductive composite materials. Because of its large aspect ratio and superior electrical properties, the electrical percolation can be achieved by addition of only a small amount of graphene in polymers.[8−10] Therefore, graphene is one of the most promising candidates in polymer composites that can be used as conductive, antistatic, and electromagnetic interference shielding materials.[11,12]

Since large-scale production of high-quality graphene is still a challenge, an increasing number of researchers focus on further decreasing the percolation threshold of graphene-filled polymers, in other words, using less graphene to achieve higher electrical conductivity. One effective method is to improve the quality of graphene and make the graphene more uniformly distributed in the polymer matrices.[13,14] However, it is known that the percolation threshold of polymer/graphene composites depends not only on the physical properties of graphene (e.g., conductivity and aspect ratio) as well as its dispersion degree but also on its distribution state in polymer matrices. Therefore, another effective method is to optimize the state of the aggregation and distribution of graphene in polymers by making the graphene selectively located in any one phase of a cocontinuous immiscible polymer blend; therefore, the percolation threshold can be significantly reduced which can be attributed to the double percolation phenomenon. The concept of double percolation is first proposed by Sumita et al.[15] in the carbon black (CB) filled immiscible polymer blends. In that work, they observed that CB was predominantly distributed in one phase of the blends or concentrated at the interfaces of the two polymers with a cocontinuous structure, which has significant improvement on the electrical conductivity of polymer composites. Subsequently, this double percolation concept has been applied to a number of polymer blends with a variety of carbon-based fillers such as CB,[16−18] carbon nanotubes (CNTs),[19−21] and carbon fibers (CFs).[22] For example, Göldel et al.[23] investigated polycarbonate (PC)/poly(styrene-acrylonitrile) (SAN)/multiwalled carbon nanotube (MWNT) composites and observed that the MWNTs were exclusively located within the PC phase, regardless of different mixing procedures, resulting in much lower electrical resistivities as compared to PC or SAN composites with the same MWNT content. Besides the selectivity of nanofillers in polymer blends, the phase continuity of the cocontinuous structure also plays an important role for the electrical properties of conductive nanoparticles filled polymer blends.

Received: July 4, 2012
Accepted: September 5, 2012
Published: September 5, 2012

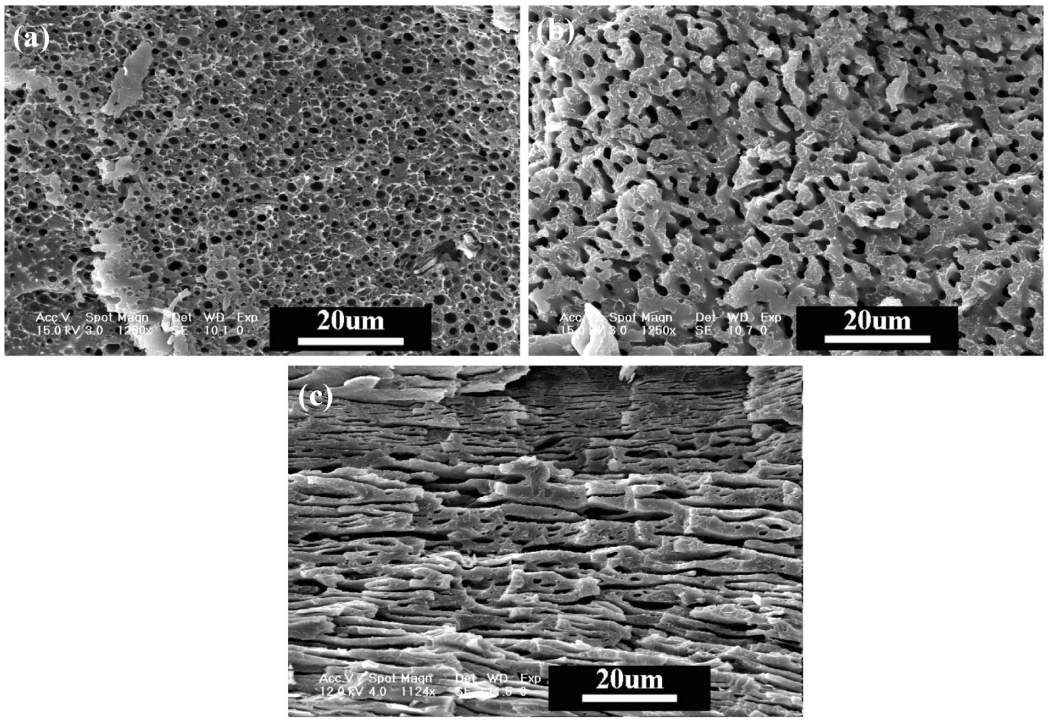

Figure 1. SEM images of PS/PMMA blends filled with 1.0 wt % GE-ODA: (a) 70w/30w, (b) 50w/50w, (c) 30w/70w. (a and b) PMMA phase was etched by formic acid. (c) PS phase was etched by cyclohexane.

For instance, Yuan et al.[24] examined the effect of phase morphology on the electrical properties of MWNT filled low density polyethylene (LDPE)/poly(vinylidene fluoride) (PVDF) composites and observed a significantly reduced percolation threshold in a double percolated structure compared to the MWNT-filled single LDPE composites. Recently, Vlemincks et al.[25] reported that thermally induced phase separation of poly[(α-methyl styrene)-co-(acrylonitrile)]/poly(methyl-methacrylate) blends in the presence of thermally reduced graphene can lead to a transformation of blends from insulating materials to highly conducting materials. This phenomenon may be attributed to the formation of three-dimensional graphene-rich domains, i.e. double percolation structure. However, systematic investigation of the influence of double percolation effect on the electrical properties is absent in that work.

Although considerable efforts have been contributed to design the electrical conductive polymer composites filled with various carbon-based fillers using the concept of double percolation, to the best of our knowledge, the concept of double percolation was seldom applied to the graphene-filled immiscible polymer blends, and so far, there is still lack of a comprehensive understanding of double percolation effect on the electrical properties of graphene-filled polymer composites. Since the high conductivity of graphene, it can be predicted that graphene-filled cocontinuous polymer blends can offer much higher electrical properties than other carbon-based fillers filled cocontinuous polymer blends. In the current study, polystyrene (PS)/poly(methyl methacrylate) (PMMA) immiscible blends are selected as host matrices to fill the octadecylamine-functionalized graphene (GE-ODA). The dependence of the electrical properties of the composites on the phase morphology and graphene content is investigated systematically. The structures and morphologies of the PS/PMMA/GE-ODA nanocomposites are visualized by scanning electron microscopy (SEM) and transmission electron microscopy (TEM). The TEM images confirm that the GE-ODA is selectively located in the PS phase. The electrical conductivity measurements reveal that the PS/PMMA/GE-ODA composite at a PS/PMMA weight ratio of 50/50 (w/w) displays a dramatically reduced percolation threshold (2.0 → 0.5 wt %) compared to the PS/GE-ODA composite due to the double percolation phenomenon. Moreover, rheological measurements are also performed to detect the percolating GE-ODA network, which can establish the relationship between microstructure and electrical properties of the GE-ODA filled composites. Our results provide a simple and effective way to markedly reduce the loading content of graphene in the polymer composites to achieve the electrical percolation using the concept of double percolation.

2. EXPERIMENTAL SECTION

2.1. Materials. The two types of immiscible polymers used are PS and PMMA. PS (J110, Vestyron) was obtained from Hüls AG, Marl, Germany. PMMA (IF850) was purchased from LG, Korea. Octadecylamine-functionalized graphene used in this work was obtained by modifying graphene oxide with octadecylamine (ODA) and then reducing it by hydroquinone. The detailed description for the preparation and characterization of GE-ODA was given in the Supporting Information.

2.2. Preparation of PS/PMMA/GE-ODA Composites. PS/PMMA/GE-ODA composites were prepared by solution blending. First, PS and PMMA were dissolved in tetrahydrofuran (THF) at 45 °C. The predetermined amount of GE-ODA was dispersed in THF (0.5 mg/mL) and exfoliated by bath sonication (KQ3200DE, 150 W) at room temperature for 1 h. Then, the suspension of GE-ODA was combined with the PS/PMMA solution to yield a total composite mass of 1.6 g. After constant mechanical stirring for 3 h, the solution was slowly added dropwise into a large volume of ethanol to coagulate the composites with vigorous stirring. The precipitate was filtered and dried in vacuum at 80 °C for 24 h. Moreover, the neat PS and PMMA and the unfilled PS/PMMA blends were also prepared in the same

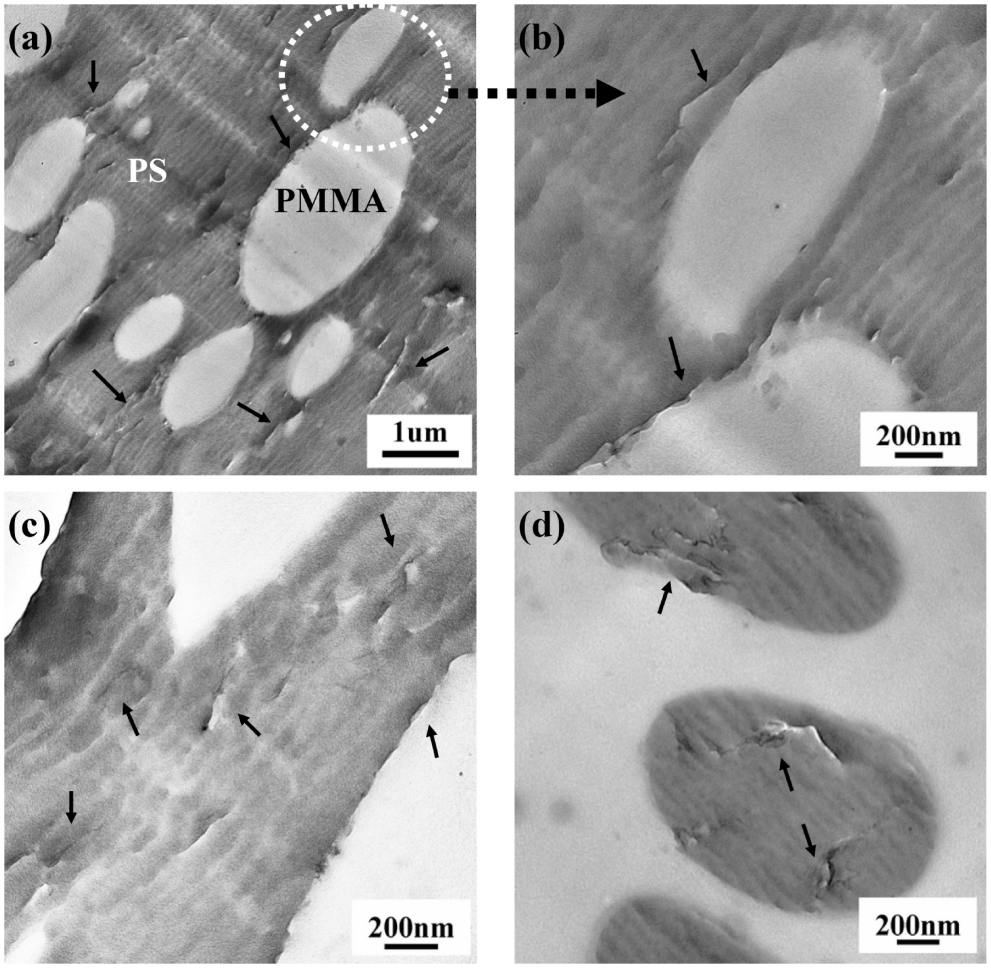

Figure 2. TEM images of PS/PMMA blends filled with 1.0 wt % GE-ODA: (a) 70w/30w, (b) partial enlarged image of part a, (c) 50w/50w, and (d) 30w/70w. The black arrows point to GE-ODA.

procedures. Finally, sheet samples for further measurement were made by hot-pressing into 25 mm diameter and 0.8 mm thick plates at ca. 200 °C and ca. 10 MPa for 10 min.

2.3. Measurement and Characterization. *2.3.1. Scanning Electron Microscopy.* SEM measurements were performed on a XL30 ESEM (FEG, Micrion FEI PHILIPS) accelerating voltage of 100 kV. For preparing the SEM samples, specimens were first fractured in liquid nitrogen. Then the PMMA phases were etched by formic acid for 1 h while the PS phases were etched by cyclohexane for 10 h. Subsequently, the etched samples were sputter-coated with a thin layer of gold.

2.3.2. Transmission Electron Microscopy. TEM measurements were performed on a JEOL JEM-1011 transmission electron microscopy operated at an acceleration voltage of 100 kV. Samples were cut to ultrathin films at room temperature by a microtome (LEICA ULTRACUTR ME_1-057) equipped with a glass knife.

2.3.3. Electrical Conductivity Measurements. The alternating-current (AC) conductivity was measured at room temperature in the frequency range between 10^0 and 10^6 Hz using an Alpha high performance frequency analyzer coupled to a Novocontrol Broadband Dielectric Spectrometer. The surface of the samples was painted with silver paste to ensure good contact.

2.3.4. Rheological Measurements. Rheological measurements were carried out on an ARES-G2 Rheometer (TA Instruments) using a parallel plate geometry with 25 mm diameter plates at 200 °C in a nitrogen atmosphere. The measurements were performed in dynamic mode with setting the gap at 0.7 mm. The strain amplitude was kept at 1%, which is within the linearity limit. The frequency sweep was then performed from 100 to 0.01 rad/s.

3. RESULTS AND DISCUSSION

3.1. Morphology of PS/PMMA/GE-ODA Ternary Composites. SEM measurements were carried out to characterize the phase morphologies of the PS/PMMA/GE-ODA ternary composites. Figure 1 shows the SEM images of the PS/PMMA blends with 1.0 wt % GE-ODA but at different PS/PMMA ratios. For the PS/PMMA composites at 70w/30w (Figure 1a) and 50w/50w (Figure 1b), the PMMA phases were etched by formic acid. Instead, the PS phases were etched by cyclohexane for the composites at 30w/70w of PS and PMMA. From Figure 1a, one can observe a typical sea-island structure for the 70w/30w PS/PMMA blend, i.e., the PMMA spherical domains are dispersed in the PS matrix. Once the percentage of PMMA in the blends increases to 50 wt %, however, a cocontinuous structure is well developed, as shown in Figure 1b. For the 30w/70w PS/PMMA blend, the PS forms a layer-like structure and almost connects with each other whereas PMMA remains a continuous structure, as shown in Figure 1c. This orientation may be induced by the shear flow during the hot-pressing process. From Figures 1a–c, it is clear that we can tune the structure and morphology of the PS/PMMA/GE-ODA composites by adjusting the component ratios of the two immiscible polymers.

The distribution of graphene in polymers was characterized by the TEM technique. In Figure 2, we present the TEM images of the PS/PMMA/GE-ODA blends (1.0 wt % GE-

dx.doi.org/10.1021/am301230q | ACS Appl. Mater. Interfaces 2012, 4, 5281–5286

ODA) at different PS/PMMA ratios. A typical two-phase structure can be observed in Figure 2, in which the light and dark parts correspond to PMMA and PS phases, respectively. From Figure 2, it is clear that most GE-ODA nanosheets are selectively dispersed in PS phase while only a few GE-ODA nanosheets are located at the phase interface. No GE-ODA nanosheets are observed in PMMA phase, whatever the PS is the dispersed phase or continuous phase. In addition, GE-ODA nanosheets are uniformly dispersed in PS phase without agglomeration. The selective localization behavior is mainly caused by the difference in the affinity and polarity between GE-ODA and the two polymer components. When graphene is functionalized by octadecylamine, the long nonpolar octadecyl chains graft onto the graphene surface, which makes it hydrophobic. Thus, the nonpolarity of GE-ODA and $\pi-\pi$ interactions between GE-ODA and PS are the main reasons that cause the selectivity of GE-ODA in PS.

3.2. Electrical Conductivity. According to the concept of double percolation, the phase continuity, i.e. the phase morphology of the composites, plays a very important role to the electrical properties of the polymer composites. It is clear that the phase morphology can be easily tuned by adjusting the weight ratio of PS/PMMA, as what we have exhibited in Figure 1. In Figure 3, we present the measured AC conductivities (at 1 Hz) for the composites at different phase morphologies as a function of PMMA contents. The concentration of GE-ODA in the entire polymer blends is fixed at 1.0 wt %. When GE-ODA is filled into single PS (0 wt % PMMA), the PS/GE-ODA composite displays a very low conductivity, which indicates that the concentration of GE-ODA (1.0 wt %) is below its electrical percolation threshold in PS. As PMMA content increases to 30 wt %, PMMA forms a large number of spheres uniformly distributed in the PS matrix, as shown in Figure 1a. Since GE-ODA is highly selective for PS phase, the increase of PMMA content, i.e., decrease of PS content, leads to an increase of GE-ODA concentration in PS phase. As a result, a slight increase in conductivity is observed. As further increasing the PMMA content to 50 wt %, there is a 6 order of magnitude increase in the conductivity of the composite as compared to that of the PS/GE-ODA composite. This significant increase in electrical conductivity is attributed to the double percolation phenomenon. First, the PS/PMMA/GE-ODA composite forms a cocontinuous phase structure at a PS/PMMA weight ratio of 50/50, as shown in Figure 1b, which ensures the continuity of GE-ODA selected phase, i.e. PS phase. Second, sharply decreasing the PS content from 100 to 50 wt % causes a remarkable increase of GE-ODA concentration in PS phase, which ensures the GE-ODA nanosheets can form a percolated conductive network throughout the PS phase at a low GE-ODA loading. With further increasing the PMMA content to 70 wt %, the continuity of the PS phases emerges a little decrease. From the corresponding SEM image shown in Figure 1c, it is clear that the system under this circumstance forms an oriented cocontinuous morphology, which signifies that the continuity of the graphene-filled PS phase in the three-dimensional space is deficient. As a result, its AC conductivity exhibits a slight decrease. When GE-ODA is filled in single PMMA, the conductivity of the resulting composite drops remarkably because the GE-ODA concentration is lower than its percolation threshold in PMMA.

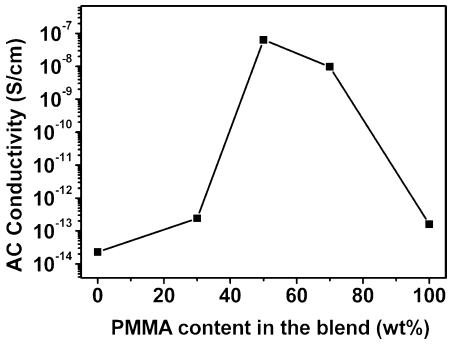

Figure 3. AC conductivity (at 1 Hz) vs PMMA content in PS/PMMA blends. The measurements were performed at room temperature. The total weight concentration of GE-ODA incorporated in the entire polymer blends is fixed at 1.0 wt %.

The electrical conductivity of composites is also highly related to the loading of the fillers. In Figure 4, we present the variation of the AC conductivities (at 1 Hz) of the composites of PS/GE-ODA, PMMA/GE-ODA, and PS/PMMA/GE-ODA (PS/PMMA: 50w/50w) as a function of GE-ODA content. From Figure 4, the electrical conductivities of both PS/GE-ODA and PMMA/GE-ODA composites display an obvious improvement with increasing the loading of GE-ODA. At the same loading of GE-ODA, however, PS/PMMA (50w/50w) composite exhibits a much higher conductivity than that of the neat PS and PMMA composites. Moreover, it is worthy to note that the electrical percolation threshold of the PS/GE-ODA composites is in the range of 1.5 and 2.0 wt %, whereas the percolation in PMMA/GE-ODA composites occurs when the filler concentration reaches to 2.0 wt %. However, the percolation threshold of PS/PMMA/GE-ODA composite is near by 0.5 wt %, which is approximately a quarter of that of the binary composites. As what we have discussed in the previous sections, this remarkable decrease in percolation threshold is ascribed to the double percolation effect.

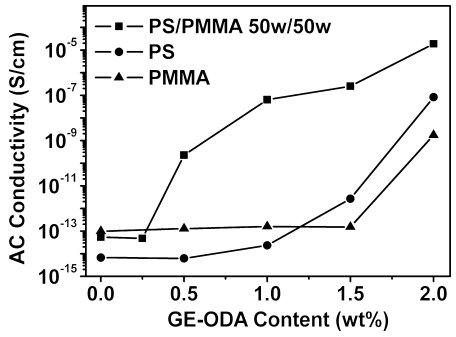

Figure 4. AC conductivity (at 1 Hz) vs GE-ODA loading in PS/PMMA (50w/50w) blend, single PS, and single PMMA. The measurements were performed at room temperature.

3.3. Rheology. The rheology of polymer–nanoparticle composites is very sensitive to the particulate microstructure, which makes the rheometry one of the most sensitive methods to probe this microstructure. For example, a typical low-frequency plateau for the storage moduli can be observed when the fillers form a space-filling particulate network.[26−28]

Figure 5 shows the variation in storage modulus (G') as a function of angular frequency (ω) for the PS/GE-ODA, PMMA/GE-ODA, and PS/PMMA/GE-ODA (PS/PMMA: 50w/50w) composites at different GE-ODA contents. For all the samples, G' gradually increases with increasing the

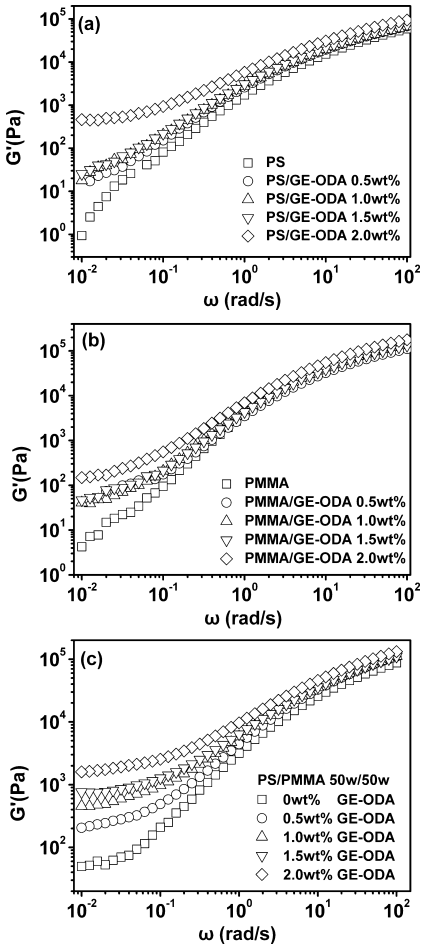

Figure 5. Storage modulus (G') as a function of frequency (ω) for PS (a), PMMA (b), and 50w/50w PS/PMMA blend (c) with varied GE-ODA content.

graphene content. This is a typical behavior for all the particles-filled polymers.[29−31] A much stronger increase in G' is observed at low frequencies, which suggests that a graphene network is gradually developing as graphene content increases. When the graphene content reaches to 2.0 wt %, both PS/GE-ODA (Figure 5a) and PMMA/GE-ODA (Figure 5b) composites show a pronounced low-frequency plateau in the $G'-\omega$ curves. However, the pronounced low-frequency plateau is observed for PS/PMMA/GE-ODA composites when the content of GE-ODA is as low as 0.5 wt % (Figure 5c). The presence of low-frequency plateau of G' indicates that these samples contain a percolating particulate network, i.e. graphene network here.[32−34] Clearly, the percolation threshold in rheology agrees well with the percolation threshold in the electrical conductivity shown in the above section. Comparing Figure 5 parts a−c, it is notable that the G' value of the neat PS/PMMA blend is a little higher than that of pure PS and pure PMMA. The storage moduli of the blend deviates from classical terminal behavior which can be attributed to the high degree of interconnectivity and network structure formed in the cocontinuous blend.[35,36]

To investigate the effect of phase morphology on the graphene network, the variation of storage modulus with angular frequency for the PS/PMMA/GE-ODA (1.0 wt % GE-ODA) composites at different ratios of PS to PMMA is presented in Figure 6. In the low-frequency region, the 50/50

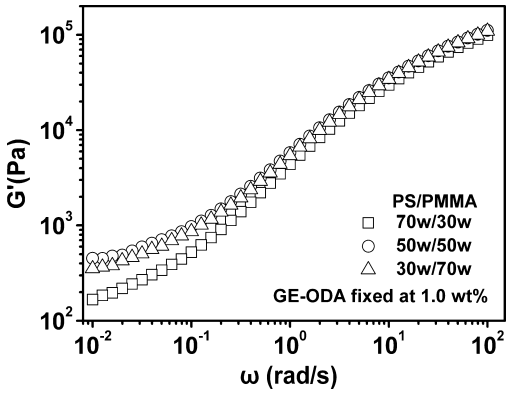

Figure 6. Storage modulus (G') as a function of frequency (ω) for the PS/PMMA blends at different ratios of PS to PMMA. The content of GE-ODA is fixed at 1.0 wt %.

blend exhibits a little higher G' value than that of the 30/70 blend, whereas the 70/30 blend shows the lowest G' value. For the 70/30 blend, PMMA phases disperse in the PS matrix. The increase of low-frequency G' is mainly contributed by the aggregate of GE-ODA in PS matrix. For the 50/50 and 30/70 blends, PS and PMMA form the cocontinuous phase morphology and GE-ODA builds a percolating network in the PS phase. As a result, the samples of 50/50 and 30/70 blends display a much higher low-frequency G' in $G'-\omega$ curves. Since the phase continuity of 50/50 blend is better than that of the 30/70 blend, as shown in Figure 1b and c, its low-frequency G' is slightly higher than that of the 30/70 blend. This tendency of rheological properties is in good accordance with the electrical properties of the samples, i.e., the electrical properties of the samples from high to low in sequence is the 50/50 blend, the 30/70 blend, and the 70/30 blend.

4. CONCLUSIONS

In this study, the concept of double percolation was applied to design the graphene filled electrical conductive materials. By adjusting the proportion of PS and PMMA, we fabricated the PS/PMMA/GE-ODA composites with double percolated structure, namely, GE-ODA selectively distributed and formed continuous conductive channels within the PS phase, and both PS and PMMA phases were cocontinuous throughout the samples. Due to the double percolation effect, the PS/PMMA (50w/50w) blend filled with GE-ODA has excellent electrical conductivity, which exhibits the lowest percolation threshold (ca. 0.5 wt %). The rheological properties of the composites were also measured to probe the microstructure of graphene aggregate as well as the phase morphology, which provides a deeper understanding of dependence of the electrical properties of composites on the phase morphology. Our results imply that the incorporation of graphene into immiscible polymer blends is an efficient way to improve the electrical properties, which offers a new route to design the conductive nanocomposites by adjusting the phase morphology of the polymer blends.

■ ASSOCIATED CONTENT

Ⓢ Supporting Information

Methods used to synthesize GE-ODA, and the FTIR, XPS, TEM, AFM, and electrical conductivity characterizations for GE-ODA. This material is available free of charge via the Internet at http://pubs.acs.org.

AUTHOR INFORMATION

Corresponding Author

*E-mail: ytzhu@ciac.jl.cn (Y.Z.); wjiang@ciac.jl.cn (W.J.). Telephone: +86-43185262866. Fax: +86-43185262126.

Notes

The authors declare no competing financial interest.

ACKNOWLEDGMENTS

This work was financially supported by the National Natural Science Foundation of China for Youth Science Funds (21104083), Major Program (50930001), and the Scientific Development Program of Jilin Province (201201007).

REFERENCES

(1) Lee, C.; Wei, X. D.; Kysar, J. W.; Hone, J. *Science* **2008**, *321*, 385−388.
(2) Balandin, A. A.; Ghosh, S.; Bao, W. Z.; Calizo, I.; Teweldebrhan, D.; Miao, F.; Lau, C. N. *Nano Lett.* **2008**, *8*, 902−907.
(3) Du, X.; Skachko, I.; Barker, A.; Andrei, E. Y. *Nat. Nanotechnol.* **2008**, *3*, 491−495.
(4) Eda, G.; Chhowalla, M. *Nano Lett.* **2009**, *9*, 814−818.
(5) Wang, D. W.; Li, F.; Zhao, J. P.; Ren, W. C.; Chen, Z. G.; Tan, J.; Wu, Z. S.; Gentle, I.; Lu, G. Q.; Cheng, H. M. *ACS Nano* **2009**, *3*, 1745−1752.
(6) Zhu, Y.; Murali, S.; Stoller, M. D.; Ganesh, K. J.; Cai, W.; Ferreira, P. J.; Pirkle, A.; Wallace, R. M.; Cychosz, K. A.; Thommes, M.; Su, D.; Stach, E. A.; Ruoff, R. S. *Science* **2011**, *332*, 1537−1541.
(7) Shan, C. S.; Yang, H. F.; Han, D. X.; Zhang, Q. X.; Ivaska, A.; Niu, L. *Langmuir* **2009**, *25*, 12030−12033.
(8) Stankovich, S.; Dikin, D. A.; Dommett, G. H. B.; Kohlhaas, K. M.; Zimney, E. J.; Stach, E. A.; Piner, R. D.; Nguyen, S. T.; Ruoff, R. S. *Nature* **2006**, *442*, 282−286.
(9) Kuila, T.; Bose, S.; Hong, C. E.; Uddin, M. E.; Khanra, P.; Kim, N. H.; Lee, J. H. *Carbon* **2011**, *49*, 1033−1037.
(10) Potts, J. R.; Murali, S.; Zhu, Y.; Zhao, X.; Ruoff, R. S. *Macromolecules* **2011**, *44*, 6488−6495.
(11) Liang, J. J.; Wang, Y.; Huang, Y.; Ma, Y. F.; Liu, Z. F.; Cai, F. M.; Zhang, C. D.; Gao, H. J.; Chen, Y. S. *Carbon* **2009**, *47*, 922−925.
(12) Zhang, H. B.; Yan, Q.; Zheng, W. G.; He, Z.; Yu, Z. Z. *ACS Appl. Mater. Interfaces* **2011**, *3*, 918−924.
(13) Barroso-Bujans, F.; Boucher, V. M.; Pomposo, J. A.; Buruaga, L.; Alegria, A.; Colmenero, J. *Chem. Commun.* **2012**, *48*, 2618−2620.
(14) Wu, H.; Zhao, W. F.; Hu, H. W.; Chen, G. H. *J. Mater. Chem.* **2011**, *21*, 8626−8632.
(15) Sumita, M.; Sakata, K.; Asai, S.; Miyasaka, K.; Nakagawa, H. *Polym. Bull.* **1991**, *25*, 265−271.
(16) Al-Saleh, M. H.; Sundararaj, U. *Compos. A* **2008**, *39*, 284−293.
(17) Gubbels, F.; Jerome, R.; Teyssie, P.; Vanlathem, E.; Deltour, R.; Calderone, A.; Parente, V.; Bredas, J. L. *Macromolecules* **1994**, *27*, 1972−1974.
(18) Calberg, C.; Blacher, S.; Gubbels, F.; Brouers, F.; Deltour, R.; Jerome, R. *J. Phys. D: Appl. Phys.* **1999**, *32*, 1517−1525.
(19) Li, Y. J.; Shimizu, H. *Macromolecules* **2008**, *41*, 5339−5344.
(20) Khare, R. A.; Bhattacharyya, A. R.; Kulkarni, A. R.; Saroop, M.; Biswas, A. *J. Polym. Sci., Part B: Polym. Phys.* **2008**, *46*, 2286−2295.
(21) Pötschke, P.; Bhattacharyya, A. R.; Janke, A. *Polymer* **2003**, *44*, 8061−8069.
(22) Thongruang, W.; Spontak, R. J.; Balik, C. M. *Polymer* **2002**, *43*, 3717−3725.
(23) Göldel, A.; Kasaliwal, G.; Pötschke, P. *Macromol. Rapid Commun.* **2009**, *30*, 423−429.
(24) Yuan, J. K.; Yao, S. H.; Sylvestre, A.; Bai, J. B. *J. Phys. Chem. C* **2012**, *116*, 2051−2058.
(25) Vleminckx, G.; Bose, S.; Leys, J.; Vermant, J.; Wübbenhorst, M.; Abdala, A. A.; Macosko, C.; Moldenaers, P. *ACS Appl. Mater. Interfaces* **2011**, *3*, 3172−3180.
(26) Krishnamoorti, R.; Yurekli, K. *Curr. Opin. Colloid Interface Sci.* **2001**, *6*, 464−470.
(27) Solomon, M. J.; Almusallam, A. S.; Seefeldt, K. F.; Somwangthanaroj, A.; Varadan, P. *Macromolecules* **2001**, *34*, 1864−1872.
(28) Zhu, Y. T.; Cardinaels, R.; Mewis, J.; Moldenaers, P. *Rheol. Acta* **2009**, *48*, 1049−1058.
(29) Carreau, P. J.; Lavoie, P. A.; Bagassi, M. *Macromol. Symp.* **1996**, *108*, 111−126.
(30) Aral, B. K.; Kalyon, D. M. *J. Rheol.* **1997**, *41*, 599−620.
(31) Le Meins, J. F.; Moldenaers, P.; Mewis, J. *Ind. Eng. Chem. Res.* **2002**, *41*, 6297−6304.
(32) Du, F. M.; Scogna, R. C.; Zhou, W.; Brand, S.; Fischer, J. E.; Winey, K. I. *Macromolecules* **2004**, *37*, 9048−9055.
(33) Zhang, Q. H.; Fang, F.; Zhao, X.; Li, Y. Z.; Zhu, M. F.; Chen, D. J. *J. Phys. Chem. B* **2008**, *112*, 12606−12611.
(34) Bose, S.; Özdilek, C.; Leys, J.; Seo, J. W.; Wübbenhorst, M.; Vermant, J.; Moldenaers, P. *ACS Appl. Mater. Interfaces* **2010**, *2*, 800−807.
(35) Li, R. M.; Yu, W.; Zhou, C. X. *J. Macromol. Sci. Part B: Phys.* **2006**, *45*, 889−898.
(36) Li, R. M.; Yu, W.; Zhou, C. X. *Polym. Bull.* **2006**, *56*, 455−466.